The Effect of Zeolite/Chitosan Hybrid Matrix for Thermal-stabilization Enhancement on the Immobilization of *Aspergillus fumigatus* α-Amylase

Yandri Yandri [1*], Hendri Ropingi [1], Tati Suhartati [1], John Hendri [1], Bambang Irawan [2], Sutopo Hadi [1]

[1] *Department of Chemistry, Lampung University, Lampung, Indonesia.*

[2] *Department of Biology, Lampung University, Lampung, Indonesia.*

Abstract

In this paper, the *A. fumigatus* α-amylase had been immobilized onto zeolite/chitosan hybrid to improve its thermal-stabilization for industrial needs. The methods applied enzyme production, isolation, partial purification, immobilization, and characterization. The optimum temperatures of the native and immobilized enzymes were 50 and 55°C, respectively. The native enzyme has KM of 3.478 ± 0.271 mg mL^{-1} substrate and V_{max} of 2.211 ± 0.096 μmole mL^{-1} min^{-1}, while the immobilized enzyme has KM value of 12.051 ± 4.949 mg mL^{-1} substrate and V_{max} of 1.602 ± 0.576 μmole mL^{-1} min^{-1}. The residual activity of the immobilized enzyme retained up 10.97% after fifth reuse cycles. The native enzyme has ΔG_i of 104.35 ± 1.09 kJ mole^{-1} and t½ of 38.75 ± 1.53 min, while the immobilized enzyme has ΔG_i of 108.03 ± 0.05 kJ mole^{-1} and t½ of 180.03 ± 3.31 min. According to the increase in half-life (t½), stability improvement of the *A. fumigatus* α-amylase was 4.65 times greater than the native enzyme. Thus, the zeolite/chitosan hybrid is used as a new supporting matrix for further enzyme immobilization to stabilize the enzymes.

1- Introduction

Enzyme is well known as biocatalyst which supports the green chemistry program in transforming the sustainable and renewable natural resources. Enzyme is more profitable to be widely used in industry by the following advantages: biodegradable, environmental friendly, high specificity and selectivity, well worked at mild conditions, low toxicity, reduce production time and costs, and may improve the product [1, 2]. The enzyme market has gained recognition globally from 10 billion US dollars in 2019 to 14.7 billion US dollars in 2025. In 2022, the highest demand of the worldwide enzyme market will be in Asia Pacific (40%) followed by North America, and Europe. A number of enzymes have been involved in the global market; including amylases, proteases, lipases, polymerases, and nucleases [3-5].

The α-amylase (E.C.3.2.1.1, α-1, 4-glucan-4-glucanohydrolase) breaks the α-1, 4 glycosidic bonds down in the starch polymers, resulting the glucose, maltose, and maltotriose [6]. This enzyme is valuable in a broad range of industrial applications ranging from foods and beverages, chemicals, pharmaceuticals, medical devices, biosensors, paper and pulp, leather, textiles, detergents, cosmetics, animal feed, biofuel, and biodiesel industries [7, 8]. The α-amylase enzyme can be isolated extracellular from several microorganisms, both bacteria and fungi. *Bacillus* and *Aspergillus* genus are often used as the host α-amylase enzymes on industrial scale. Global production of α-amylase from *B. licheniformis* and *Aspergillus sp.* were around 300 tons [4]. Microbial α-amylase is one of the most influential industrial amylases, occupying approximately 25% of the global enzyme market [9]; for instance, the annual cost of α-amylase in the starch

---

industry was about 62.2 million US dollars [10]. In this research, the α-amylase was isolated from *Aspergillus fumigatus* which can adapt to various organic compounds for its metabolic processes and does not show special nutritional needs [11].

Similar problems relating to thermal instability have been identified with most industrial enzymes, especially during applications in batch processes. These include easy water solubility, a higher tendency for denaturation under greater temperatures, the possibility of being contaminated with other substances in a reaction, and the fact that they can only be used once in a process. In addition, the starches need a high temperature to be processed on an industrial scale. One of the powerful methods to enhance the enzyme stability, reusability, and properties is by the immobilization [12]. The use of immobilized enzymes on an industrial scale has several advantages, as follows: thermostable, rigid, easy to regenerate, repeatedly used, does not contaminate the product, facilitates the reaction control process, biocompatible, and presence of reactive functional groups [13].

In the current study, the *A. fumigatus* α-amylase was immobilized onto a zeolite/chitosan hybrid matrix as the newest matrix type for thermal-stabilization enhancement. The hydroxyl and amine groups in a zeolite/chitosan hybrid structure may undergo the non-covalent interaction to the enzymes by forming the hydrogen bonds [14]. Thus, this immobilization method is based on the presence of physical adsorption which has some benefits, such as: does not affect to the enzyme conformation, the enzyme is easily separated from the matrix, and the matrix can be regenerated [15]. Furthermore, the zeolite matrix contains the heterogeneous surface to strengthen non-covalent interactions with the enzymes, while the chitosan was chosen as a matrix by the following properties: economics, abundant raw material, has good adhesion and mechanical strength [16-18].

Nowadays, some experiments of the hybrid matrices formed by various materials are being investigated to improve the material properties include as an adsorbent, catalyst, or supporting matrix on the enzyme immobilization. The hybrid of chitin-bentonite observed in recent studies confirmed the presence of elevated adsorption capacity compared to samples where pure bentonite and chitin served as adsorbents [19]. Likewise, the hybrid matrices were confirmed to be the better matrix than the classic material on the enzyme immobilization. For instance, the immobilization of the *A. fumigatus* α-amylase onto a bentonite matrix increased its thermal stability 2.9 times according to the growth of half-life [20]. Meanwhile, the *A. fumigatus* α-amylase immobilized on a chitin/bentonite hybrid matrix has greater thermal stability about 3.8 times than the native form, and maintained 72% of its initial activity after incubating at 60°C for 80 min [21]. Furthermore, the cellulase immobilized onto a TiO_2/lignin hybrid had a half-life (113.61 min) five times the values recorded for the native variant (433.13 min). Hence, the hybrid was determined to demonstrate relatively better thermal stability compared to an unmodified lignin [22]. Similar finding, the immobilized glucose oxidase on a zeolite/chitosan hybrid matrix showed the stability improvement against microbial activity [23]. Furthermore, the immobilized α-amylase onto a bentonite/chitosan hybrid could be reused for fifth cycles and retained up 87 % of its residual activity [24].

The hybrid matrix also showed some contrasting benefits against processes where classic material were used as catalysts, especially in an attempt to ensure the matrix properties are improved, alongside an increase the thermal-stabilization of enzyme [13]. The interaction between hybrid matrix and the enzyme will be more stable, mechanically resistant, well worked at mild conditions, reusable, and prevent the conformational changes during storage [25, 26]. Based on it, this pioneering study analyzed the use of zeolite/chitosan hybrid as a supporting matrix to optimize the thermal-stabilization stability of the *A. fumigatus* α-amylase by immobilization procedure. Therefore, the temperature dependence, kinetic and thermodynamic parameters, and reusability of the immobilized *A. fumigatus* α-amylase were examined for the first time to measure quantify of its stability improvement. This study suggests a protocol for the production of highly stable and reusable biocatalytic systems for practical application in the starch hydrolysis. This research information is important, as it can be used as a basis for further development in the search for reusable and applicable hybrid matrix for producing immobilized enzyme on industrial scale.

2- Materials and Methods

2-1- Materials

The Microbiology Laboratory, Biology Department, Lampung University, provided the locally sourced fungi isolate *A. fumigatus*. Zeolite (particle size: < 45 μm) and glutaraldehyde (50 wt. in H_2O) were purchased from Sigma-Aldrich, while chitosan (DD: 95.22%) was purchased from CV. ChiMultiguna, and all chemical reagents were of analytical grade.

2-2- Production and Isolation of the α-amylase

The enzyme isolation and partial purification were according to an earlier study [21], whereas the local fungal isolate was cultivated in Potato Dextrose Agar medium which consist of 0.1% corn starch as an inducer. The crude enzyme was produced from *A. fumigatus* through Sub-merged Fermentation at 32°C for 112 hours, containing: $(NH_4)_2SO_4$ 1.4%,

KH_2PO_4 2.0%, $MgSO_4.7H_2O$ 0.3%, urea 0.3%, $CaCl_2$ 0.3%, $FeSO_4.7H_2O$ 0.005%, $ZnSO_4.7H_2O$ 0.0014%, $CoCl_2$ 0.002%, corn starch 0.75%, and peptone 0.75% in a 0.05 M phosphate buffer pH 6.5. The crude enzyme was isolated from the fermentation broth by centrifugation at 5000 rpm for 15-20 min. The flowchart of the research is presented in Figure 1.
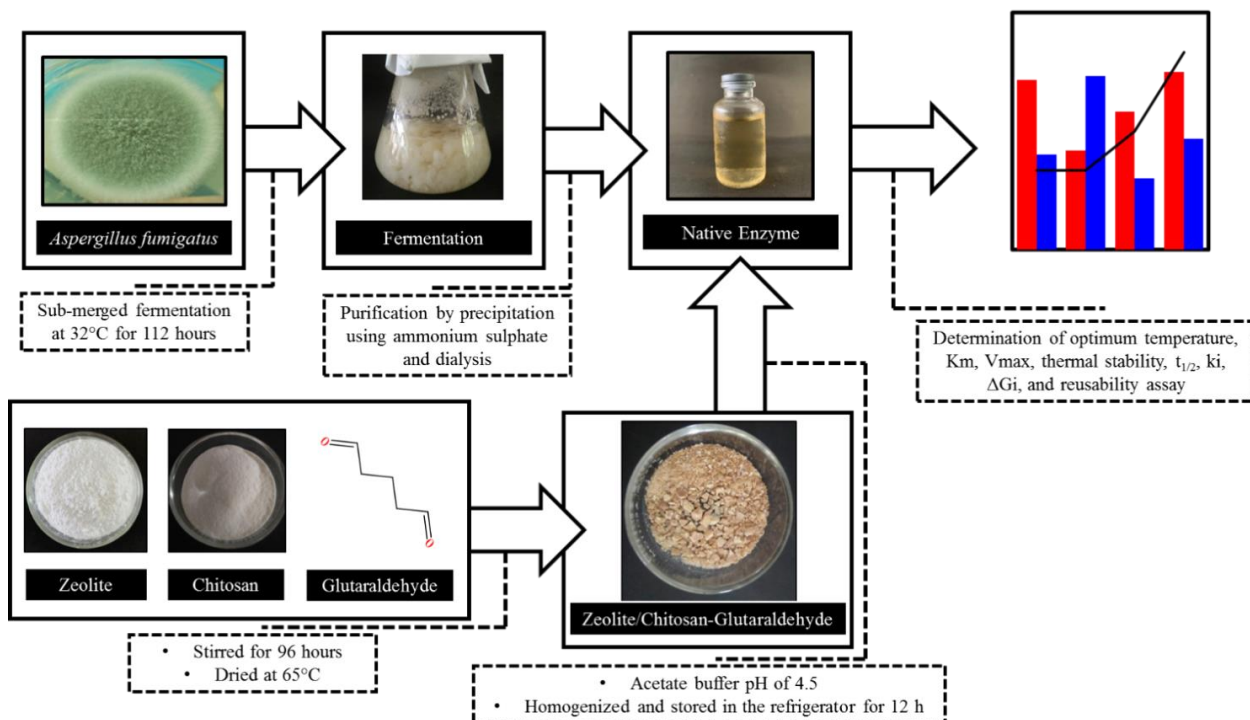

Figure 1. Flowchart of the research methodology

2-3- Purification of the α-Amylase

The partial purification of crude enzymes was achieved by precipitation with ammonium sulfate as well as dialysis [27]. The crude enzyme was partially purified by ammonium sulphate in an ice bath. Furthermore 0-20% saturation level was attained with the crude enzyme by using ammonium sulphate. Then the precipitate removal was achieved through centrifugation for 15-20 min at 5,000 rpm, before introducing ammonium sulphate into the supernatant. This process ensured saturation levels in the range of 20-85% was achieved [20]. The precipitated protein (enzyme) was separated from its filtrate by centrifuging for 15 min at 5000 rpm, temperature of 4°C, and consequently dissolved in sufficient quantity of phosphate buffer (0.025 M; pH 6.5). Furthermore, the suspension of enzymes was subjected to dialysis, using a dialysis bag (8000 Da) through the night on phosphate buffer (0.01 M; pH 6.5) and set at 4 °C [20].

2-4- Analysis of α-Amylase Activity and Determination of Protein Content

The Fuwa method was applied to evaluate the activities exhibited by α-amylase enzymes the partial purification process was. This involved adding iodine reagent proportionate to the substrate amount reduced within a 10 min incubation time [28], while characterization steps, based on Mandel's method, involved applying dinitrosalicylic acid reagent, and was centered on glucose (reducing sugar) concentration[29]. The protein content in purification steps was determined based on the Lowry method [30].

2-5- Zeolite/chitosan Preparation

The chitosan powder, measuring 2.0 g, was added to 1% acetic acid (100 mL) and stirred to ensure dissolution for about 4 hours. Then, a 2.0 g of zeolite was added, followed by 100 mL of distilled water. Next, 4 mL of 1 M NaOH and 100 mL of filtered water were added subsequently, and then stirred for 68 hours. After that, 160 μL of glutaraldehyde was added and mixed for 24 hours. Finally, the hybrid matrix was dried in the oven at 65°C [31]. Furthermore, the laboratory mill was used to ground the dried matrix before sieving, then functional groups were determined using FT-IR spectroscopy, by analyzing about 5g of zeolite/chitosan hybrid powder at wavenumber ranging from 4000-650 cm^{-1} [20].

2-6- Immobilization of Native Enzyme

A total of 0.2 g of zeolite/chitosan matrix was washed by a 0.1 M acetate buffer pH 4.5. Then, 0.5 mL of native enzyme was added, then stored in the refrigerator for 12 hours [31, 32]. The enzyme activity was assayed using Mandel's method.

2-7- Optimum Temperature Determination

The parameter evaluated to determine the optimum temperature of both immobilized and native enzymes was residual activity (%). This analysis was performed after the samples were incubated at different temperatures, namely 45; 50; 55; 60; 65; 70; 75; and 80°C. Hence, the particular temperature with the most significant enzyme activity was considered to be optimal.

2-8- Determination of KM Dan V_{max} Values

Some of the kinetic parameters, comprising Michaelis constant (K_M) and maximum velocity (V_{max}) were evaluated applying the Lineweaver–Burk plot. This assessment was carried out on experimental data demonstrating an interaction between enzyme activities and starch substrates under the ensuing concentration scope: 0.1; 0.2; 0.4; 0.6; 0.8; and 1.0%. In addition, both native and immobilized enzymes were then incubated at respective optimal temperatures for 30 min, before subjecting to assay through the Mandel's method. The existence of a proportional correlation between enzyme-catalysed reaction rate and enzyme activity was established. The Lineweaver-Burk plot (Equation 1) was used to determine the K_M and V_{max} values, as shown below:

$$\frac{1}{v} = \frac{1}{V_{max}} + \frac{K_M}{V_{max}} \times \frac{1}{[S]} \qquad (1)$$

where K_M is Michaelis constant; V_{max} is maximum reaction rate; v is initial reaction rate; and $[S]$ is substrate concentration. K_M value was determined as the optimum substrate concentration for subsequent procedures [15].

2-9- Thermal Stability Determination

Thermal stability of the native and immobilized enzymes were selected from the residual activity retainment after inactivation at 60°C at the following inactivation time (t_i) variations: 0, 10, 20, 30, 40, 50, 60, 70, and 80 min [33, 34]. The enzyme activity was assayed by Mandel's method, and this data was applied to define k_i, $t_{1/2}$, and ΔG_i values. The residual activity is determined by Equation 2:

$$\text{Residual activity } (\%) = \frac{E_i}{E_o} \times 100\% \qquad (2)$$

where E_o is the residual activity at t_o; and E_i is the residual activity at t_i [34].

2-10- Determination of $t_{1/2}$, k_i, and ΔG_i

The first demand enzyme inactivation rate Equation 3 was used to calculate the half-life ($t_{1/2}$) and thermal inactivation rate constant (k_i):

$$\ln\left(\frac{E_i}{E_o}\right) = - k_i \times t_i \qquad (3)$$

where k_i signifies thermal inactivation rate constant; E_i was the residual activity at t_i; E_o denotes the residual activity at t_o; and t_i represents thermal inactivation time [35]. In addition, the k_i was determined as the graph slope $ln\frac{[E]_i}{[E]_o}$ against t_i

Therefore, free energy resulting from denaturation (ΔG_i) was described as a prerequisite for enzyme denaturation. This value was further estimated based on the following thermodynamic Equation 4:

$$\Delta G_i = \text{-RT } \ln\frac{k_i.h}{k_b.T} \qquad (4)$$

where ΔG_i is the free energy conversion due to denaturation; T is the thermal inactivation temperature (K); R is the ideal gas constant; k_i is the thermal inactivation rate constant; h is the Planck constant, and k_B is the Boltzman constant [35].

2-11- Reusability Assay

The immobilized enzymes previously responded with starch substrate were subsequently rewashed by centrifugation applying a 0.1 M acetate buffer solution of pH 4.5. The product was further reacted a second time using fresh substrate [20, 36] before Mandel's method was applied to define the α-amylase activity. Furthermore, the entire procedure was carried out in five replicates.

2-12- Statistical Analysis

Duplicate determination was performed for all samples (n = 2), and the data obtained were documented in the form of a mean ± standard deviation (SD). Therefore, the possible significant differences between replicates were evaluated using the student t-test (Paired Two Sample for Means), alongside ANOVA analysis. The findings were believed to be significant at $p < 0.05$ to reject the null hypothesis. This indicates the absence of any differences between the two replicates.

3- Results and Discussion

3-1- The α-Amylase Purification

In purification steps, the α-amylase activity to hydrolyse the starch substrate was emphasized to the starch-iodine or reducing sugar value methods. The enzyme unit activity was evaluated using 0.1 % soluble starch in distilled water (pH ± 6.5), which performed for 10 min at a temperature of 60°C. In addition, crude enzyme isolates obtained from *A. fumigatus* demonstrated a specific activity of 568.07 U/mg, which was subsequently purified partially by precipitations of ammonium sulphate at the percent saturations of (0-20)% and (20-85)%, as shown in Figure 2 Based on the Figure 2, the enzyme precipitate by the (20-85)% ammonium sulphate had specific activity of 2151.69 U/mg. As a comparison, the *A. fumigatus* α-amylase in the latest research was partially purified by (20-85)% ammonium sulphate and its typical activity was 3970.08 U/mg [20].
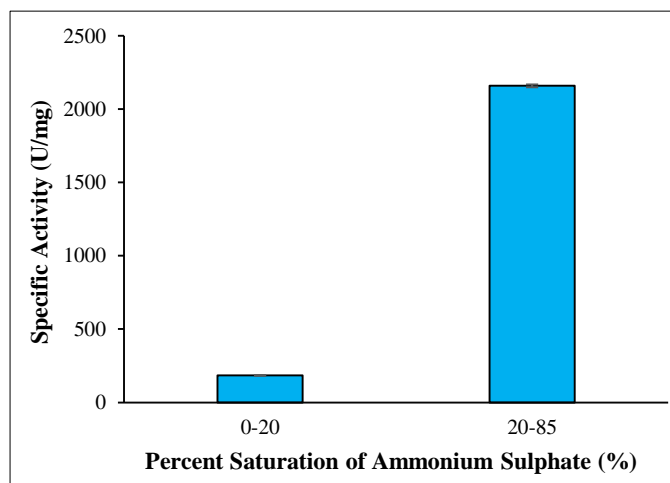

Figure 2. The relationship between (0-20)% and (20-85)% saturation of ammonium sulfate on the enzyme specific activity

The enzyme fraction (20-85)% was purified by dialysis overnight using 0.01 M phosphate buffer pH 6.5. After dialysis, the enzyme revealed significant growth in its purity than the crude enzyme which show by the higher of its specific activity. The dialyzed enzyme had specific activity of 8237.09 U/mg. Table 1 summarizes the outcome of this partial purification step. This result shows a 14.5 increase in enzyme purity compared to the crude variant. Furthermore, these characteristics were supported by the relative decline in enzyme yield (%) which implied that the enzyme was free from impurities, especially the salt ions and other proteins. As a comparison in a previous literature, the specific activity of the dialyzed *A. fumigatus* α-amylase was 4514.67 U/mg [20]. Hence, this present study was successfully improved the purity and catalytic activity of the *A. fumigatus* α-amylase.

Table 1. Partial purification procedures summary of *A. fumigatus* α-amylase

Step	Volume	Unit activity	Protein content	Specific activity	Total activity	Purity	Yield
	(mL)	(U mL^{-1})	(mg mL^{-1})	(U mg^{-1})	(U)	(x-fold)	(%)
Crude enzyme	4000	116.90	0.2058	568.07	467593.76	1.0	100.00
Fraction (NH$_4$)$_2$SO$_4$ (20-85)%	400	559.25	0.2599	2151.69	223701.12	3.8	47.84
Dialysis	900	191.60	0.0233	8237.09	172441.73	14.5	36.88

3-2- Fourier Transform Infrared (FTIR) Spectrometry Analysis

The FTIR spectra of zeolite, chitosan, and zeolite/chitosan hybrid matrices are given in Figure 3. The FTIR spectrum of zeolite in the range of 1200-450 cm^{-1} was corresponded to the T-O-T layers (T= Si and Al) [37]. Another peak at 1001.06 cm^{-1} was contributed to the Si-O, Al-O, and Si-O-Al stretching in the tetrahedral layer [38]. The bands at 1656.85 cm^{-1} and 3429.43 cm^{-1} were corresponded to the water molecules in its cavity and O-H groups, respectively [39, 40]. In contrast, corresponding region between 1422 and 603 cm^{-1} in the FTIR spectrum of chitosan was confirmed as the CH$_3$, CH$_2$, CH, and O-H groups attached to the pyranose ring [41]. The peaks at 1606.70 and 2922.16 cm^{-1} revealed the existence of N-H and C-H bending [42, 43]. A broadband at 3448 cm^{-1} was corresponded to the intermolecular hydrogen bonds by the NH$_2$ and O-H groups [44]. On another hand, the FTIR spectrum of zeolite/chitosan hybrid showed both combination of functional groups in zeolite and chitosan. T-O bending and double ring vibration at 464.84 and 553.57 cm^{-1} did not change. Likewise, the band at 3429.43 cm^{-1} corresponded to the O-H stretching was still exist. However, there was the band shift from 1421.54 to 1,425.40 cm^{-1} contributed to the CH$_3$ stretching, from 2922.16 to 2937.59 cm^{-1} corresponded to the CH, and from 667.37 to 671.23 cm^{-1} corresponded to the symmetrical stretching in zeolite [45-47]. This is due to the overlap of the zeolite-chitosan structures through the active siloxane group in the

zeolite [48]. The peak at 1627 cm^{-1} revealed the existence of a C=N imine group from the cross-linking between glutaraldehyde and chitosan [49]. According to the previous research, chitosan adsorption on zeolite results from electrostatic attraction of anionic zeolite on cationic chitosan [23].
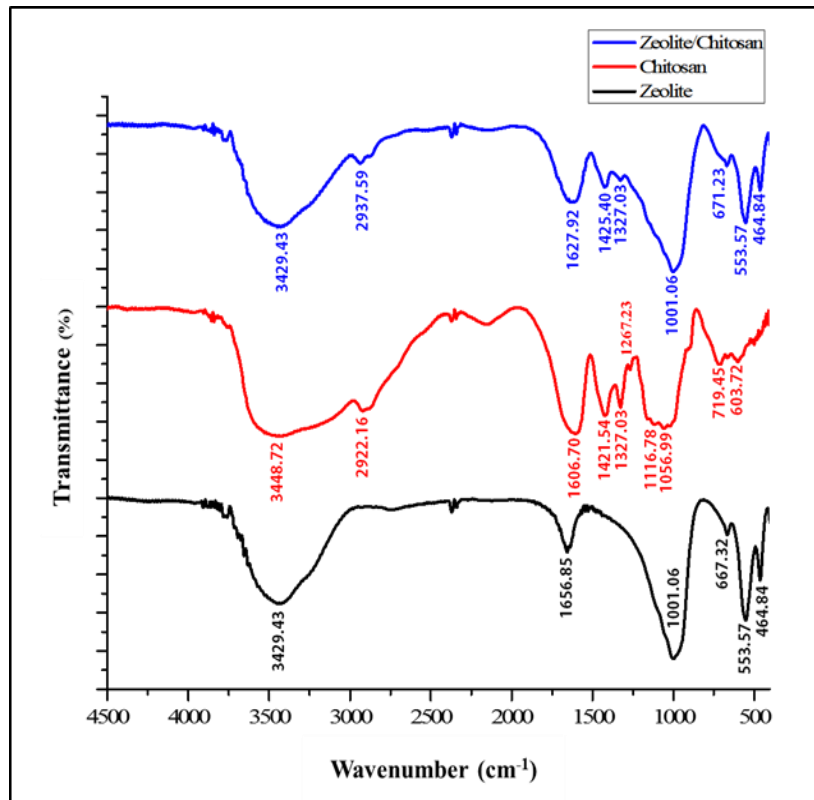

Figure 3. FTIR spectra of zeolite, chitosan, and zeolite/chitosan

3-3- Determination of Binding PH and Optimum Temperature

There are numerous process parameters known to affect the immobilized enzymes' ability to degrade starch substrate, including temperature and pH. Based on previous research, acidic pH media were determined to create a more suitable environment for α-amylase to bind onto zeolite/chitosan matrix. The enzyme molecules were positively charged under the immobilization condition provided by an acetate buffer set at pH 4.5. This set-up initiates biocatalyst immobilization, which occurs predominantly through ionic and electrostatic interactions. At the optimum temperature, the substrate and enzyme molecules will have an ideal kinetic energy to optimize the collisions whereas the catalysed reaction rate is optimum. Thus, the enzyme's active site opens to interact with the substrate behind incubation at its optimum temperature to form the enzyme-substrate complex [50]. The optimum temperature for the native and immobilized enzymes is illustrated in Figure 4.
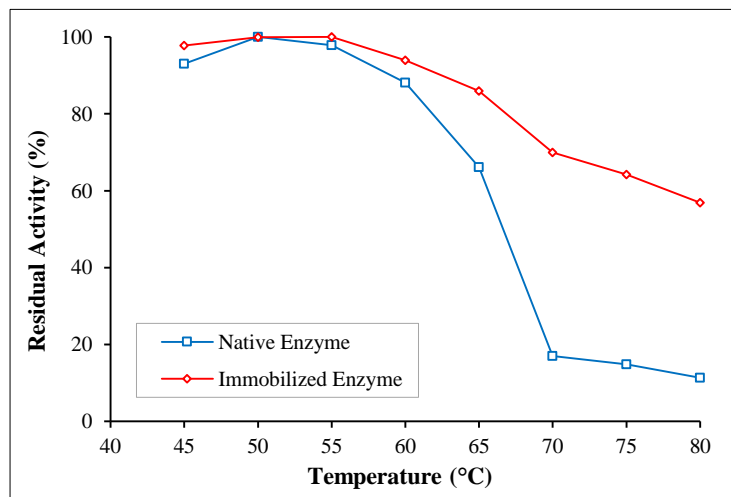

Figure 4. Different temperatures effects on the native and immobilized enzymes activities (mean ± SD; n = 2; p < 0.05)

As presented in Figure 4, the native enzyme has optimum temperature of 50°C, while the immobilized enzyme has higher temperature of 55°C. The optimum temperature shift indicated that the immobilized enzyme was more thermostable compared to the native enzyme because of the matrix protection to the enzyme molecules [51]. Similar finding was recorded by Klapiszewski et al. [22] who was reported that the immobilized *A. oryzae* α-amylase onto TiO$_2$/lignin hybrid matrix revealed the most elevated activity at 55-60°C optimum temperature. Furthermore, the immobilized enzyme activity was higher at extreme temperatures after 60°C compared to the native form so that it was more thermo-stable than the native form. According to the graph, the activity of enzymes under the specified temperature was anticipated. However, further increase in temperature elevated the intrinsic activity to attain an optimum reaction temperature and was consequently overlapped with enzyme deactivation. In conclusion, the use of zeolite/chitosan hybrid matrix is suitable option for thermal-stabilization enhancement of the *A. fumigatus* α-amylase when applied to batch process at extreme temperature.

3-4- Determination of K_M and V_{max}

The kinetic parameters, including K_M and V_{max} values, determined for the two enzyme forms were assessed to verify the effect of immobilization on enzyme affinity with substrate molecules, as well as their catalytic efficiency. This evaluation was calculated using a Lineweaver–Burk plot, estimated to show the linear association between *1/[S]* and *1/V*. However, the rate (V) of product formation is assumed to depend solely on substrate availability *[S]*. The correlation between reaction rate (V) and substrate concentration *[S]* is dependent on the enzyme affinity for the substrate (K_M) [15]. Figure 5 shows the Lineweaver–Burk plot of both immobilized and native enzymes, while Table 2 represents the respective K_M and V_{max} values. Furthermore, Michaelis constant (K_M) depicts the enzyme affinity for a particular substrate, while maximum velocity (V_{max}) assesses the magnitude of this activity. A change in the substrate concentration was also practiced to analyse the study kinetics *[S]*, ranging from 2.0 to 10.0 mg/mL for both native and immobilized enzymes at each optimum temperature.
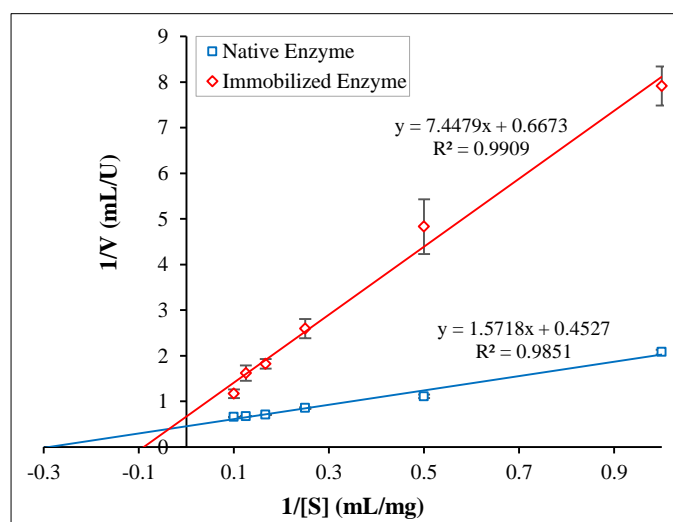

Figure 5. Lineweaver-Burk plot of the native and immobilized enzymes (mean ± SD; n = 2; p < 0.05)

Table 2. Kinetic parameters for the native and immobilized α-amylase in the latest experiments

Matrix Type	K_M		V_{max}		Ref.
	Native enzyme	Immobilized enzyme	Native enzyme	Immobilized enzyme	
Bentonite/chitosan hybrid	43.56 g L^{-1}	46.10 g L^{-1}	20.58 U/mg	28.17 U/mg	[24]
Bentonite	6.18 mg mL^{-1}	12.19 mg mL^{-1}	909.09 μmol mL^{-1} min^{-1}	88.5 mol mL^{-1} min^{-1}	[36]
TiO$_2$/lignin hybrid	11.04 mM	15.03 mM	920 U/mg	855 U/mg	[51]
Chitosan	1.63 mg mL^{-1}	3.51 mg mL^{-1}	39.68 μmole mL^{-1} min^{-1}	7.05 μmole mL^{-1} min^{-1}	[52]
Zeolite/chitosan hybrid	3.478 ± 0.271* mg mL^{-1}	12.051 ± 4.949* mg mL^{-1}	2.211 ± 0.096* μmole mL^{-1} min^{-1}	1.602 ± 0.576* μmole mL^{-1} min^{-1}	This study

* Values were shown as mean ± SD, n = 2

Table 2 showed greater K_M with the immobilized enzyme compared to the native variant. This outcome attributes the samples with K_M to the potential for low substrate affinity, indicating the need for additional substrate concentrations, possibly reaching V_{max}. Consequently, a significant decline in reaction rate (p < 0.05) was observed with the immobilized enzyme, compared to the native variant. Similar results was found in some experiments as described in Table 2. The increased K_M after immobilization revealed that the enzyme required a higher substrate *[S]* to acquire the maximum rate (V_{max}) and the affinity of the enzyme for the substrate decreased compared to the native enzyme. Higher K_M results in

decreased enzyme affinity, caused by reduced substrate accessibility to the enzyme's active site and by enzyme structural modifications after immobilization procedure by the presence of matrix. It may also be caused by decreased diffusion, steric hindrance, and ionic strength [53]. Otherwise, the V_{max} of the immobilized enzyme appeared slightly lower, which suggests a subtle decline in starch substrate hydrolysis rate after an effective immobilization. This is potentially attributed to the occurrence of diffusional substrate restrictions to the active sites of enzymes. Another notable inference for lower V_{max} was explained based on the incident of conformational changes observed after enzyme molecules engage in non-covalent interactions with the functional groups on a matrix [54].

3-5- Determination of Thermal Stability

The thermal stability of both samples was evaluated on the basis of individual residual activity following an incubation period of 80 min and maintained at 60 °C without a substrate. Figure 6 shows the outcome of this assessment, where a significant upsurge in stability at ($p < 0.05$) was observed in the immobilized specimen. This indicates a relatively higher intrinsic residual activity. The residual activity of the native enzyme after being inactivated at 60°C for 80 min was retained up 21.50%, while the immobilized enzyme had maintained 72.28%. After incubation, the two enzyme samples demonstrated a significant decline in enzymatic activity from the initial levels. However, the immobilized variant exhibited a profile with lower thermal degradation as well as better heat tolerance following an 80 min incubation period.
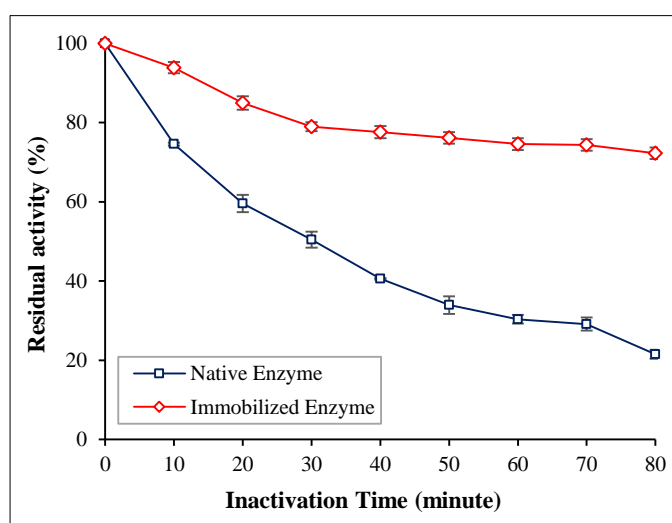

Figure 6. Thermal stability of the native and immobilized enzymes at 60°C (mean ± SD; n = 2; p < 0.05)

The conformational structure of enzymes during immobilization is potentially altered. This initiates intrinsic changes in stability and activity. Moreover, the immobilized enzyme demonstrated relatively greater stability, which is attributed to the protective effects of hybrid matrices compared to enzyme structure denaturation influenced by punitive temperature conditions. This outcome was promoted by the occurrence of interactions between matrix and enzymes, which ultimately stabilizes the complete enzyme structure immobilization. The zeolite/chitosan hybrid delivered supplementary external linkages to the individual molecules. This limits the incidence of conformational changes potentially resulting from the impact of heat, and consequently help maintain proper enzyme tertiary structure [13]. In the adsorption method, some functional groups in zeolite layer, including Si-O, Al-O, Si-O-Al, and OH groups interact with the enzyme molecules through the hydrogen bonds, electrostatic interactions, hydrophobic interactions, and Van der Waals forces [55]. Lysine and arginine residues have the most possibility to interact closely with the zeolite surface, thereby increasing the enzyme stability [56]. In the crosslinking method, the amine groups in chitosan and enzyme were cross-linked using glutaraldehyde to form the covalent bonds [57]. The O-H groups may also strengthen the interaction between chitosan and enzyme molecules via adsorption [58, 59]. The hybrid matrix could confer a protecting effect to the enzyme molecules so that the immobilized enzyme has higher thermal stability and become more rigid and has a higher resistance on thermal denaturation than the native enzyme [22].

More recent literature reported similar issues in the aspect of thermal stability, particularly at greater temperatures. The *A. fumigatus* α-amylase immobilized onto a bentonite matrix was more stable at elevated temperatures compared to the native form. They reported that immobilized enzyme maintained 56% of initial activity when disclosed at 60°C for 80 min [20]. Meanwhile, the immobilized *A. fumigatus* α-amylase onto chitin/bentonite hybrid matrix maintained 70% of initial activity at 60°C after 80 min of heating [21], implying that the hybrid matrix is a better matrix for raising the thermal stability of *A. fumigatus* α-amylase as compared to the classical matrix. In conclusion, the zeolite/chitosan hybrid in this present study had successfully improved the thermal stability of *A. fumigatus* α-amylase compared to the latest immobilization experiment using chitin/bentonite hybrid.

3-6- Determination of $t_{1/2}$, k_i, and ΔG_i

Figure 7 showed the thermal stability assay, where both samples showed residual activities and the data plotted in a graph representing first-order enzyme inactivation rate. The slope of graph in Figure 7 is expressed as a thermal inactivation rate constant (k_i), and this value was used to calculate the value of half-life ($t_{1/2}$) and the free energy conversion due to denaturation (ΔG_i) as summarized in Table 3, As a result, thermal stabilization of the immobilized enzyme was successfully improved which was observed by a significant ($p < 0.05$) decline of k_i, the rise of its half-life ($t_{1/2}$) and the increase of ΔG_i compared to the native enzyme. A decline in the k_i of immobilized enzymes showed reductions in the denaturation rate resulting from low water flexibility. Therefore, higher stability is anticipated following the folding structural conformation [35].
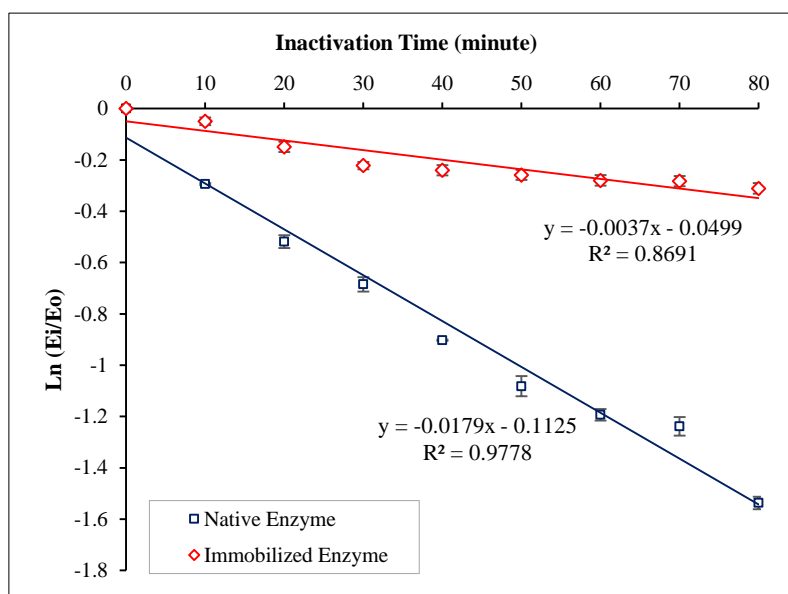

Figure 7. First-order inactivation rate plot of the native and immobilized enzymes at 60°C (mean ± SD; n = 2; p < 0.05)

Table 3. $t_{1/2}$ and ΔG_i values for native and immobilized α-amylase in the latest experiments

Host Enzyme	Matrix	Half-life ($t_{1/2}$) (min)		The transformation of free energy because denaturation (ΔG_i) (kJ mole^{-1})		Stability Improvement	Ref.
		Before	After	Before	After		
A. fumigatus	Bentonite	40.53 ± 1.9001*	115.50 ± 5.7895*	104.47 ± 0.1296*	107.37 ± 0.1386*	2.9	[20]
A. fumigatus	Bentonite/Chitin hybrid	40.53 ± 1.9001*	154.00 ± 13.3963*	104.47 ± 0.1296*	108.17 ± 0.2389*	3.8	[21]
B. subtilis ITBCCB148	Bentonite	42	88.85	104.57	106.65	2.12	[36]
B. subtilis ITBCCB148	Chitosan	113.61	433.13	107.34	111.06	3.8	[51]
A. fumigatus	Zeolite/Chitosan hybrid	38.75 ± 1.53*	180.03 ± 3.31*	104.35 ± 1.09*	108.03 ± 0.05*	4.65	This study

* Values were shown as mean ± SD, n = 2

The term "half-life ($t_{1/2}$)" depicts the period during which half the enzyme activity is inactivated [35]. Therefore, higher values of immobilized enzymes indicate a 4.65 times increase in thermal stabilization in contrast with the native variants. This characteristic elongates the time for enzyme inactivation and loss of activity, thus denoting better stability. The native variant is easily degraded at greater temperatures, and consequently yields a decline in half-life values. This outcome is attributed to enzyme denaturation and thermal degradation, but the immobilized enzyme was could maintain its activity and stability from the denaturation effect. In contrast, the smaller ΔG_i of the native enzyme indicated a spontaneous thermal denaturation process, while the higher ΔG_i of the immobilized enzyme indicated the folding conformation raise in tertiary structure of the immobilized enzyme. Hence, the enzyme conformation became more rigid, stable, and less flexible in the water. Thus, the energy needed for denaturation became more increased. The denaturation may loss the hydrogen bond's strength and Van der Waals interactions [35]. As compared to other experiments in Table 3, the zeolite/chitosan hybrid in this present study had successfully increased the half-life of *A. fumigatus* α-amylase compared to the latest immobilization experiments using other classical matrices, resulting the best stability improvement of the enzyme.

3-7- Reusability Study

The reusability of immobilized enzymes is the most important features for economically industrial application. The immobilized enzyme exhibits the advantage of being repeatedly used on fresh substrates. Figure 8 showed the test for

reusability, which was conducted five times under optimum conditions. According to the graph, the immobilized enzyme could be used in fifth cycles and maintained 10.97% of its activity, while the reuse of it directed to the significant ($p <$ 0.05) decline of its activity. The decline in activity was because of the loss of enzyme after rewashed. This outcome was further clarified by enzyme inactivation resulting from denaturation and the consequent leakage.
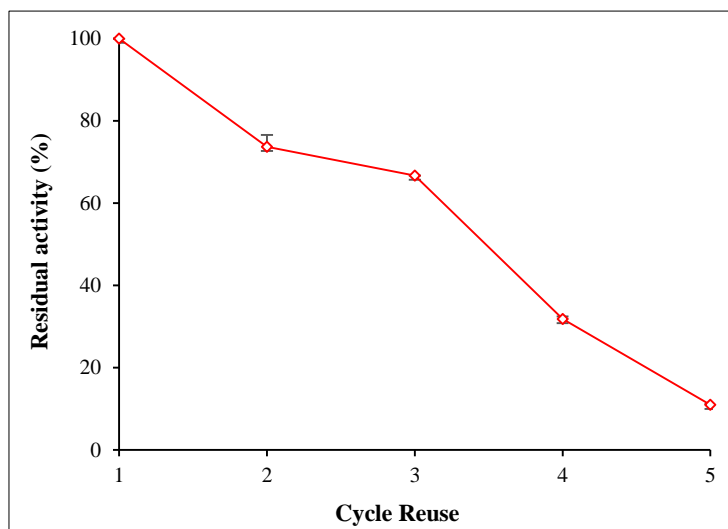

Figure 8. Reusability assay of the immobilized enzyme (mean ± SD; n = 2; p < 0.05)

Reusability study for immobilized α-amylase in the latest experiments than the present data was summarized in Table 4. The study result shows better thermal resistance and stability during reactions conferred on the biocatalysts by the hybrid matrix. Also, the system was observed to have better reuse potentials, efficiency, purity and overall quality. The enzymes are also protected against conformational changes under storage conditions, and the enzymes tend to be easier to separate from the matrix [13]. Hence, the immobilized enzyme can be utilized in industrial applications without significant loss of its properties over several cycles. The enzyme reusability in this present study is still need to be improved in the next research for economically industrial application.

Table 4. Reusability study for immobilized α-amylase in the latest experiments

Host Enzyme	Matrix Type	Reuse Cycles	Residual Activity (%)	Ref.
A. fumigatus	Bentonite	6	42	[20]
A. fumigatus	Bentonite/chitin hybrid	6	36	[21]
B. subtilis	Chitosan/bentonite hybrid	5	87	[24]
B. subtilis	Bentonite	6	40	[36]
A. niger	TiO$_2$/lignin hybrid	10	90	[51]
B. subtilis	Chitosan	6	16	[52]
A. fumigatus	Zeolite/chitosan hybrid	5	11	This study

4- Conclusion

The immobilization of the *A. fumigatus* α-amylase onto zeolite/chitosan hybrid matrix successfully increased of its thermal stability, reusability, and properties. The findings indicate *A. fumigatus* α-amylase has an optimum temperature of 55°C which is higher than the native enzyme and become thermo-stable. Then, an acidic pH (acetate buffer at pH 4.5) was suitable for binding the α-amylase onto the zeolite/chitosan hybrid. The K_M and V_{max} values were slightly changed after the immobilization process. The significant higher K_M observed in immobilized enzymes showed a decline in affinity for the substrate. Therefore, higher substrate quantities were required to attain the maximum rate (V_{max}), in contrast with the native variant. In particularly, the K_M and V_{max} of the immobilized enzymes were 12.051 ± 4.949 mg mL^{-1} and 1.602 ± 0.576 μmole mL^{-1} min^{-1}, respectively.

The immobilized enzyme has k_i of 0.0037 min^{-1}, ΔG_i of 108.03 ± 0.05 kJ mole^{-1}, and $t_{1/2}$ of 180.03 ± 3.31 min. Based on increasing of its half-life, thermal-stabilization of the immobilized enzyme rose 4.65 times that of the native enzyme; There was substantial progress in both the chemical and thermal stability of the immobilized α-amylase, as relative activity greater than 72.28% was recorded after an 80 min incubation period. However, over 10.97% of the starting activity was retained after the five hydrolysis cycles were consecutively completed. This characteristic authenticates operational stability and is considered highly relevant in industrial applications. Therefore, this approach provides a

simple and efficient technique for zeolite/chitosan hybrid synthesis, and potential applications as a matrix to support enzyme immobilization. The hybrid materials produced as well as the methodology applied have potential for application with other biocatalysts. This pioneering information is very important for use in further research related to the development of new commercial immobilized α-amylase that are environmentally friendly and reusable.

5- Declarations

5-1- Author Contributions

Conceptualization, Y.Y. and H.R.; methodology, Y.Y., H.R., and B.I.; software, H.R and S.H.; validation, Y.Y., T.S., J.H., B.I., and S.H.; writing—original draft preparation, Y.Y. and H.R.; writing—review and editing, Y.Y., T.S., and S.H; visualization, H.R.; supervision, Y.Y., J.H., and T.S.; project administration, Y.Y. and S.H.; funding acquisition, Y.Y. All authors have read and agreed to the published version of the manuscript.

5-2- Data Availability Statement

The data presented in this study are available in the article.

5-3- Funding

5-4- Acknowledgements

5-5- Conflicts of Interest

The authors declare that there is no conflict of interests regarding the publication of this manuscript. In addition, the ethical issues, including plagiarism, informed consent, misconduct, data fabrication and/or falsification, double publication and/or submission, and redundancies have been completely observed by the authors.

6- References

[1] Ermis, E. (2017). Halal status of enzymes used in food industry. Trends in Food Science and Technology, 64, 69–73. doi:10.1016/j.tifs.2017.04.008.

[2] Chapman, J., Ismail, A. E., & Dinu, C. Z. (2018). Industrial applications of enzymes: Recent advances, techniques, and outlooks. Catalysts, 8(6), 20–29. doi:10.3390/catal8060238.

[3] Veerana, M., Mitra, S., Ki, S. H., Kim, S. M., Choi, E. H., Lee, T., & Park, G. (2020). Plasma-mediated enhancement of enzyme secretion in *Aspergillus oryzae*. Microbial Biotechnology, 14(1), 262–276. doi:10.1111/1751-7915.13696.

[4] Thatoi, H., Mohapatra, P. K. D., Mohapatra, S., & Mondal, K. C. (2020). Microbial Fermentation and Enzyme Technology. CRC Press, Florida, United States. doi:10.1201/9780429061257.

[5] Grand View Research. (2021). Enzymes Market Size, Share & Trends Analysis Report By Type (Industrial, Specialty), By Product (Carbohydrase, Proteases), By Source (Microorganisms, Animals), By Region, and Segment Forecasts, 2021-2028. Available online: https://www.grandviewresearch.com/industry-analysis/enzymes-industry/ (accessed on January 2022).

[6] Vogel, A., & May, O. (Eds.). (2019). Industrial enzyme applications. John Wiley & Sons, New Jersey, United States. doi:10.1002/9783527813780.

[7] Basso, A., & Serban, S. (2019). Industrial applications of immobilized enzymes—A review. Molecular Catalysis, 479(110607), 1–20. doi:10.1016/j.mcat.2019.110607.

[8] Singh, R. S., Singhania, R. R., Pandey, A., & Larroche, C. (2019). Biomass, biofuels, biochemicals: advances in enzyme technology. Elsevier, Amsterdam, Netherlands. doi:10.1016/C2019-0-00323-8.

[9] Salem, K., Elgharbi, F., Ben Hlima, H., Perduca, M., Sayari, A., & Hmida-Sayari, A. (2020). Biochemical characterization and structural insights into the high substrate affinity of a dimeric and Ca2+ independent *Bacillus subtilis* α-amylase. Biotechnology Progress, 36(4), 1–14. doi:10.1002/btpr.2964.

[10] Sharma, M., Sharma, V., & Majumdar, D. K. (2014). Entrapment of α-Amylase in Agar Beads for Biocatalysis of Macromolecular Substrate. International Scholarly Research Notices, 2014, 1–8. doi:10.1155/2014/936129.

[11] Van De Veerdonk, F. L., Gresnigt, M. S., Romani, L., Netea, M. G., & Latgé, J. P. (2017). *Aspergillus fumigatus* morphology and dynamic host interactions. Nature Reviews Microbiology, 15(11), 661–674. doi:10.1038/nrmicro.2017.90.

[12] Guisan, J. M., Bolivar, J. M., López-Gallego, F., & Rocha-Martín, J. (2020). Immobilization of enzymes and cells: Methods and protocols. Humana Press, New Jersey, United States. doi:10.1007/978-1-0716-0215-7.

[13] Zdarta, J., Meyer, A. S., Jesionowski, T., & Pinelo, M. (2018). A general overview of support materials for enzyme immobilization: Characteristics, properties, practical utility. Catalysts, 8(2), 1–27. doi:10.3390/catal8020092.

[14] Mohamad, N. R., Marzuki, N. H. C., Buang, N. A., Huyop, F., & Wahab, R. A. (2015). An overview of technologies for immobilization of enzymes and surface analysis techniques for immobilized enzymes. Biotechnology and Biotechnological Equipment, 29(2), 205–220. doi:10.1080/13102818.2015.1008192.

[15] Robinson, P. K. (2015). Enzymes: principles and biotechnological applications. Essays in Biochemistry, 59, 1–41. doi:10.1042/BSE0590001.

[16] Datta, S., Christena, L. R., & Rajaram, Y. R. S. (2013). Enzyme immobilization: an overview on techniques and support materials. 3 Biotech, 3(1), 1–9. doi:10.1007/s13205-012-0071-7.

[17] Talebi, M., Vaezifar, S., Jafary, F., Fazilati, M., & Motamedi, S. (2016). Stability improvement of immobilized α-amylase using nano pore zeolite. Iranian Journal of Biotechnology, 14(1), 33–38. doi:10.15171/ijb.1261.

[18] Younes, I., & Rinaudo, M. (2015). Chitin and chitosan preparation from marine sources. Structure, properties and applications. Marine Drugs, 13(3), 1133–1174. doi:10.3390/md13031133.

[19] Perez, J. J., Villanueva, M. E., Sánchez, L., Ollier, R., Alvarez, V., & Copello, G. J. (2020). Low cost and regenerable composites based on chitin/bentonite for the adsorption potential emerging pollutants. Applied Clay Science, 194, 1–7. doi:10.1016/j.clay.2020.105703.

[20] Yandri, Y., Tiarsa, E. R., Suhartati, T., Satria, H., Irawan, B., & Hadi, S. (2022). The Stability Improvement of α -Amylase Enzyme from *Aspergillus fumigatus* by Immobilization on a Bentonite Matrix. Biochemistry Research International, 2022, 1–7. doi:10.1155/2022/3797629.

[21] Tiarsa, E. R., Yandri, Y., Suhartati, T., Satria, H., Irawan, B., & Hadi, S. (2022). The Stability Improvement of *Aspergillus fumigatus* α-Amylase by Immobilization onto Chitin-Bentonite Hybrid. Biochemistry Research International, 2022, 1–9. doi:10.1155/2022/5692438.

[22] Zdarta, J., Jędrzak, A., Klapiszewski, Ł., & Jesionowski, T. (2017). Immobilization of cellulase on a functional inorganic–organic hybrid support: Stability and kinetic study. Catalysts, 7(12), 1–7. doi:10.3390/catal7120374.

[23] Tegl, G., Stagl, V., Mensah, A., Huber, D., Somitsch, W., Grosse-Kracht, S., & Guebitz, G. M. (2018). The chemo enzymatic functionalization of chitosan zeolite particles provides antioxidant and antimicrobial properties. Engineering in Life Sciences, 18(5), 334–340. doi:10.1002/elsc.201700120.

[24] Baysal, Z., Bulut, Y., Yavuz, M., & Aytekin, C. (2014). Immobilization of α-amylase via adsorption onto bentonite/ chitosan composite: Determination of equilibrium, kinetics and thermodynamic parameters. Starch/Staerke, 66(5–6), 484–490. doi:10.1002/star.201300133.

[25] Wahab, R. A., Elias, N., Abdullah, F., & Ghoshal, S. K. (2020). On the taught new tricks of enzymes immobilization: An all-inclusive overview. Reactive and Functional Polymers, 152, 1–26. doi:10.1016/j.reactfunctpolym.2020.104613.

[26] Dwevedi, A. (2016). Enzyme Immobilization: Advances in Industry, Agriculture, Medicine, and the Environment. doi:10.1007/978-3-319-41418-8.

[27] Bollag, D. M., Rozycki, M. D., & Edelstein, S. J. (1996). Protein methods (2nd Edition). WILEY-Liss, Hoboken, United States.

[28] Fuwa, H. (1954). A new method for microdetermination of amylase activity by the use of amylose as the substrate. Journal of Biochemistry, 41(5), 583–603. doi:10.1093/oxfordjournals.jbchem.a126476.

[29] Eveleigh, D. E., Mandels, M., Andreotti, R., & Roche, C. (2009). Measurement of saccharifying cellulase. Biotechnology for Biofuels, 2(1), 1-8. doi:10.1186/1754-6834-2-21.

[30] Lowry, O. H., Rosebrough, N. J., Farr, A. L., & Randall, R. J. (1951). Protein measurement with the Folin phenol reagent. The Journal of Biological Chemistry, 193(1), 265–275. doi:10.1016/s0021-9258(19)52451-6.

[31] Marotta, A., Luzzi, E., De Luna, M. S., Aprea, P., Ambrogi, V., & Filippone, G. (2021). Chitosan/zeolite composite aerogels for a fast and effective removal of both anionic and cationic dyes from water. Polymers, 13(11), 1–11. doi:10.3390/polym13111691.

[32] Wang, W., Jiang, Y., Zhou, L., & Gao, J. (2011). Comparison of the properties of lipase immobilized onto mesoporous resins by different methods. Applied Biochemistry and Biotechnology, 164(5), 561–572. doi:10.1007/s12010-010-9157-z.

[33] Ahmed, N. E., El Shamy, A. R., & Awad, H. M. (2020). Optimization and immobilization of amylase produced by *Aspergillus terreus* using pomegranate peel waste. Bulletin of the National Research Centre, 44(1), 1–12. doi:10.1186/s42269-020-00363-3.

[34] Yang, Z., Domach, M., Auger, R., Yang, F. X., & Russell, A. J. (1996). Polyethylene glycol-induced stabilization of subtilisin. Enzyme and Microbial Technology, 18(2), 82–89. doi:10.1016/0141-0229(95)00073-9.

[35] Kazan, D., Ertan, H., & Erarslan, A. (1997). Stabilization of Escherichia coli penicillin G acylase against thermal inactivation by cross-linking with dextran dialdehyde polymers. Applied Microbiology and Biotechnology, 48(2), 191–197. doi:10.1007/s002530051037.

[36] Yandri, Suhartati, T., Yuwono, S. D., Qudus, H. I., Tiarsa, E. R., & Hadi, S. (2018). Immobilization of a-amylase from *Bacillus subtilis* ITBCCB148 using bentonit. Asian Journal of Microbiology, Biotechnology and Environmental Sciences, 20(2), 487–492.

[37] Ezzeddine, Z., Batonneau-Gener, I., Pouilloux, Y., Hamad, H., & Saad, Z. (2018). Synthetic nax zeolite as a very efficient heavy metals sorbent in batch and dynamic conditions. Colloids and Interfaces, 2(2), 1–14. doi:10.3390/colloids2020022.

[38] Wang, P., Sun, Q., Zhang, Y., & Cao, J. (2019). Synthesis of zeolite 4A from kaolin and its adsorption equilibrium of carbon dioxide. Materials, 12(9), 1–12. doi:10.3390/ma12091536.

[39] Cheng, Z. L., Li, Y. X., & Liu, Z. (2017). Novel adsorption materials based on graphene oxide/Beta zeolite composite materials and their adsorption performance for rhodamine B. Journal of Alloys and Compounds, 708, 255–263. doi:10.1016/j.jallcom.2017.03.004.

[40] de Matos Degues, K., Cypriano, M. G., Coelho, K. B., Luza, A. L., Montedo, O. R. K., de Castro, L. C., & Angioletto, E. (2018). Assessment of PCM-impregnated zeolite as a matrix for latent heat storage. Materials Science Forum, 912 MSF, 87–92. doi:10.4028/www.scientific.net/MSF.912.87.

[41] Zvezdova, D. (2010). Synthesis and characterization of chitosan from marine sources in Black Sea. Annual Proceedings," Angel Kanchev" University of Ruse, Ruse, Bulgaria 49(9.1), 65-69.

[42] Ahmad, M. Bin, Tay, M. Y., Shameli, K., Hussein, M. Z., & Lim, J. J. (2011). Green synthesis and characterization of silver/chitosan/polyethylene glycol nanocomposites without any reducing agent. International Journal of Molecular Sciences, 12(8), 4872–4884. doi:10.3390/ijms12084872.

[43] Ammar, H. O., El-Nahhas, S. A., Ghorab, M. M., & Salama, A. H. (2012). Chitosan/cyclodextrin nanoparticles as drug delivery system. Journal of Inclusion Phenomena and Macrocyclic Chemistry, 72(1–2), 127–136. doi:10.1007/s10847-011-9950-5.

[44] Chen, C., Gao, Z., Qiu, X., & Hu, S. (2013). Enhancement of the controlled-release properties of chitosan membranes by crosslinking with suberoyl chloride. Molecules, 18(6), 7239–7252. doi:10.3390/molecules18067239.

[45] Lopez-Carrizales, M., Mendoza-Mendoza, E., Peralta-Rodriguez, R. D., Pérez-Díaz, M. A., Portales-Pérez, D., Magaña-Aquino, M., … Martinez-Gutierrez, F. (2020). Characterization, antibiofilm and biocompatibility properties of chitosan hydrogels loaded with silver nanoparticles and ampicillin: an alternative protection to central venous catheters. Colloids and Surfaces B: Biointerfaces, 196, 111292. doi:10.1016/j.colsurfb.2020.111292.

[46] Menazea, A. A., Eid, M. M., & Ahmed, M. K. (2020). Synthesis, characterization, and evaluation of antimicrobial activity of novel Chitosan/Tigecycline composite. International Journal of Biological Macromolecules, 147, 194–199. doi:10.1016/j.ijbiomac.2020.01.041.

[47] Vegere, K., Kravcevica, R., Krauklis, A. E., & Juhna, T. (2020). Comparative study of hydrothermal synthesis routes of zeolite A. Materials Today: Proceedings, 33, 1984–1987. doi:10.1016/j.matpr.2020.06.326.

[48] Mostafa, M., El-Meligy, M. A., Sharaf, M., Soliman, A. T., & AbuKhadra, M. R. (2021). Insight into chitosan/zeolite-A nanocomposite as an advanced carrier for levofloxacin and its anti-inflammatory properties; loading, release, and anti-inflammatory studies. International Journal of Biological Macromolecules, 179, 206–216. doi:10.1016/j.ijbiomac.2021.02.201.

[49] Manasi, Rajesh, V., & Rajesh, N. (2015). An indigenous Halomonas BVR1 strain immobilized in crosslinked chitosan for adsorption of lead and cadmium. International Journal of Biological Macromolecules, 79, 300–308. doi:10.1016/j.ijbiomac.2015.04.071.

[50] Fernandez-Lafuente, R. (2009). Stabilization of multimeric enzymes: Strategies to prevent subunit dissociation. Enzyme and Microbial Technology, 45(6–7), 405–418. doi:10.1016/j.enzmictec.2009.08.009.

[51] Klapiszewski, Ł., Zdarta, J., & Jesionowski, T. (2018). Titania/lignin hybrid materials as a novel support for α-amylase immobilization: A comprehensive study. Colloids and Surfaces B: Biointerfaces, 162, 90–97. doi:10.1016/j.colsurfb.2017.11.045.

[52] Yandri, Y., Suhartati, T., Satria, H., Widyasmara, A., & Hadi, S. (2020). Increasing Stability of a-amylase Obtained from Bacillus subtilis ITBCCB148 by Immobilization with Chitosan. Mediterranean Journal of Chemistry, 10(2), 155–161. doi:10.13171/mjc10202002131126ysh.

[53] Mohammadi, M., Khakbaz Heshmati, M., Sarabandi, K., Fathi, M., Lim, L. T., & Hamishehkar, H. (2019). Activated alginate-montmorillonite beads as an efficient carrier for pectinase immobilization. International Journal of Biological Macromolecules, 137, 253–260. doi:10.1016/j.ijbiomac.2019.06.236.

[54] Califano, V., & Costantini, A. (2020). Immobilization of cellulolytic enzymes in mesostructured silica materials. Catalysts, 10(6), 1–31. doi:10.3390/catal10060706.

[55] Wu, L., Wu, S., Xu, Z., Qiu, Y., Li, S., & Xu, H. (2016). Modified nanoporous titanium dioxide as a novel carrier for enzyme immobilization. Biosensors and Bioelectronics, 80, 59–66. doi:10.1016/j.bios.2016.01.045.

[56] Taghizadeh, T., Ameri, A., Talebian-Kiakalaieh, A., Mojtabavi, S., Ameri, A., Forootanfar, H., Tarighi, S., & Faramarzi, M. A. (2021). Lipase@zeolitic imidazolate framework ZIF-90: A highly stable and recyclable biocatalyst for the synthesis of fruity banana flavour. International Journal of Biological Macromolecules, 166, 1301–1311. doi:10.1016/j.ijbiomac.2020.11.011.

[57] Yu, L., Yu, B., Chen, H., Shang, X., He, M., Lin, M., Li, D., Zhang, W., Kang, Z., Li, J., Wang, F., Xiao, L., Wang, Q., & Fan, J. (2021). Highly efficient artificial blood coagulation shortcut confined on Ca-zeolite surface. Nano Research, 14(9), 3309–3318. doi:10.1007/s12274-021-3394-z.

[58] A. Modenez, I., Sastre, D., C. Moraes, F., & Marques Netto, C. (2018). Influence of Glutaraldehyde Cross-Linking Modes on the Recyclability of Immobilized Lipase B from Candida antarctica for Transesterification of Soy Bean Oil. Molecules, 23(9), 2230. doi:10.3390/molecules23092230.

[59] Ribeiro, E. S., de Farias, B. S., Sant'Anna Cadaval Junior, T. R., de Almeida Pinto, L. A., & Diaz, P. S. (2021). Chitosan–based nanofibers for enzyme immobilization. International Journal of Biological Macromolecules, 183, 1959–1970. doi:10.1016/j.ijbiomac.2021.05.214.